# Tree Localization Using Integrated Heading, DBH and Ultra-Wideband for Precision Forestry

Zuoya Liu[1], Harri Kaartinen[1], Antero Kukko[1,2], Juha Hyyppa[1,2], Ruizhi Chen[3]

[1] Department of Remote Sensing and Photogrammetry, Finnish Geospatial Research Institute FGI in the National Land Survey of Finland, Vuorimiehentie 5, 02150 Espoo, Finland – firstname.lastname@nls.fi
[2] Department of Built Environment, School of Engineering, Aalto University, P.O. Box 11000, FI-00076, Aalto, Finland
[3] School of Data Science/School of Artificial Intelligence, The Chinese University of Hong Kong, Shenzhen, China

**Keywords:** Tree Localization, Heading, DBH, Ultra-Wideband, Data Fusion, Precision Forestry.

**Abstract**

Accurate tree positions play a vital role in precision forestry and environmental sciences. In this study, we propose an accurate, efficient, and adaptable method for tree localization by integrating heading, diameter at breast height (DBH), and ultra-wideband technology. The proposed method is simple to implement in different forest environments and can determine the position of each tree within a few seconds. Compared with traditional field measures, such as laser rangefinders and inclinometers, the proposed approach is more efficient. In comparison with commonly used measures, such as terrestrial laser scanning (TLS) and mobile laser scanning (MLS), the proposed method is more cost-effective and easier to implement, making it particularly suitable for natural forests that are remote from roads yet require accurate measurements. Field experiments were conducted in a managed boreal forest in southern Finland, characterized by minimal understory vegetation and good visibility, where a total of 50 trees were mapped. Experimental results indicate that the proposed method can accurately determine tree positions with an RMSE of 0.12 m and an MAE of 0.11 m.

## 1. Introduction

Accurate tree positions are increasingly used in precision forestry and environmental sciences, enabling management decisions at the individual tree level and advancing forest automation. Additionally, they are critical for forest survey and management, including determining average forest volume at national scales, estimating forest biomass at regional levels, and assessing carbon sequestration and water balance across different ecosystems, thereby contributing to both environmental and economic outcomes. Importantly, improving the accuracy and efficiency of tree position measurements in forest inventories is of great importance, as it addresses the growing practical needs for efficient forest inventory, individual tree level management, and large-scale environmental monitoring in precision forestry and environmental sciences.

To achieve this objective, a wide range of tools and technologies have been developed and implemented over the past decade. Traditional field methods, such as using a laser rangefinder, inclinometer, and compass to manually measure distances and angles, are highly accurate but time-consuming and labor intensive (Apostol et al., 2018). The use of a total station or high-grade Global Navigation Satellite System (GNSS) can improve efficiency, but these approaches still require significant effort (Edson and Wing, 2012; Farid Fauzi et al., 2016). Terrestrial laser scanning (TLS) and mobile laser scanning (MLS) provide more efficient alternatives, albeit requiring time-consuming data processing to achieve high-accuracy results (Luoma et al., 2017; Wilkes et al., 2017). Using high-density airborne laser scanning (ALS) shows great prospects for individual tree mapping (Hyyppä et al., 2022; Muhojoki et al., 2024), but has limitations including difficulty in accurately measuring trees under dense canopies and high operational costs. These challenges highlight the need for efficient, accurate, and low-cost methodologies for individual tree positioning within forest plots.

Previous studies have investigated UWB propagation under forest canopies (Anderson et al., 2013), UWB technology in GNSS compromised environments (Kai et al., 2015), and UWB positioning for moving targets (Keefe et al., 2019). More recent advancements have shown that ultra-wideband (UWB) technology has significant potential for accurate and efficient positioning of individual trees in forest environments (Li et al., 2023; Liu et al., 2025; Yuan et al., 2021). Compared with traditional field methods, such as laser rangefinders and inclinometers, UWB enables efficient data collection with decimeter-level accuracy for tree positions in forest plots. Additionally, in comparison with TLS, MLS, and ALS methods, UWB provides a more cost-effective solution. However, several challenges remain to be further explored, including improving measurement accuracy and efficiency, particularly in dense forest plots, enhancing adaptability to different forest environments, and exploring potential applications in combination with other technologies, e.g. decision making at the individual tree level.

In this study, we propose an accurate, efficient, and adaptable method for determining tree positions in forest plots by integrating heading, diameter at breast height (DBH) and ultra-wideband technology. A UWB network with 16 anchors can be rapidly deployed to cover an entire plot of approximately 50 m × 50 m, making the method adaptable to a variety of forest environments. Additionally, unlike laser scanner-based approaches such as TLS and MLS, the proposed method can achieve decimeter-level measurements of tree positions with a system cost of less than 1,000 euros, requiring only one operator and less than 3 seconds per tree, making it practical for field applications. Overall, the method consists of two main steps: (1) obtaining initial tree position estimates using UWB technology, and (2) refining these positions through stem-center correction based on the measured heading and DBH. This integration enables all measurements to be consistently referenced to a common direction, magnetic north, ensuring applicability across different survey regions. Unlike previous UWB-only approaches, the proposed method uses heading and DBH measurements to correct tree positions, mitigating positioning errors caused by signal occlusion while simultaneously improving efficiency (Li et al., 2023; Yuan et al., 2021).

This contribution has been peer-reviewed. The double-blind peer-review was conducted on the basis of the full paper.
https://doi.org/10.5194/isprs-annals-XI-1-2026-297-2026  

## 2. Materials and Methods

### 2.1 Test Site

A forest plot with an area of approximately 40 m × 50 m, located in the boreal forest zone in Tuusula, Finland (60°21'24.9"N, 25°00'36.6"E), was used to test the performance of the proposed method. The dominant tree species in this plot was Scots pine (*Pinus sylvestris*), and the average tree DBH was approximately 0.3 m, as shown in Figure 1. Additionally, the test site represents a typical managed boreal forest in Finland, characterized by minimal understory vegetation and good visibility. Therefore, it was optimal for evaluating the performance of new methods for determining tree positions under a forest canopy.


Figure 1. Overview of the forest plot used in this study and the developed prototype of the integrated heading and UWB device (H-UWB), equipped with an ultrasonic distance sensor for real-time DBH measurement and position correction.

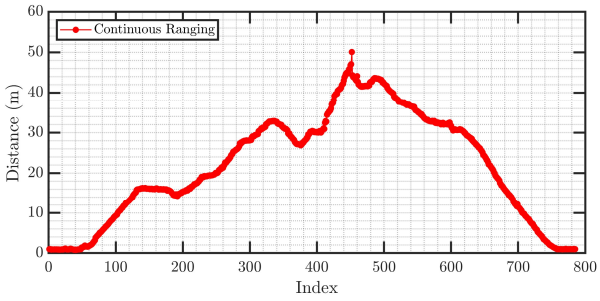


Figure 2. An example of continuous ranging between two UWB devices in the forest plot. The reliable coverage distance of the device exceeds approximately 44 m.

### 2.2 Data Collection Methods

Standalone UWB technology can also be used to determine tree positions under forest canopies, as demonstrated in studies (Sun et al., 2023; Yuan et al., 2021). However, the UWB receiver typically needs to be placed very close to the tree stem during data collection, which may introduce larger positioning errors due to signal obstruction by the stem. To mitigate this issue, multiple measurements are often conducted at different locations around the tree stem, and the average of these measurements is usually used to determine the final tree position. While this approach can reduce or even eliminate position errors, it significantly increases data collection time and is therefore not well suited for practical field surveys.

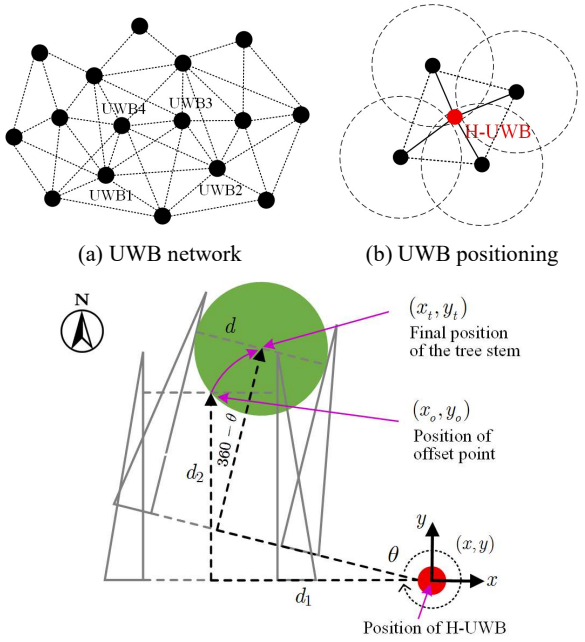


(a) UWB network (b) UWB positioning

(c) Determination of the tree stem position by integrating heading and the measured position of the H-UWB device

Figure 3. Overview of the proposed method.

To address these two issues, namely reducing the impact of tree stem occlusion on measurement accuracy and improving field efficiency, we proposed a new data collection method for determining tree positions under forest canopies by integrating heading, DBH, and ultra-wideband positioning. In this method, a total of 16 UWB devices were deployed and mounted on trees at a height of approximately 1.3-1.5 m above ground, with a random spatial distribution within the forest plot. All devices were developed based on the DW1000 chip from Qorvo and operated on Channel 2, with a reliable coverage distance exceeding approximately 44 m under forest conditions characterized by minimal understory vegetation and good visibility. Figure 2 illustrates an example of continuous distance measurements between two devices. Notably, the UWB network provided full coverage of the forest plot.

To simplify network estimation and avoid Geometric Singularity in anchor self-localization (Larsson, 2022), four devices (UWB1-UWB4) were placed at the centre of the test site with predefined relative orientations, as shown in Figure 3(a). The remaining devices were distributed around these four reference nodes. Furthermore, an integrated heading and UWB device, namely H-UWB, was developed to collect all raw data, as shown in Figure 1. The H-UWB device was developed based on the DW1000 UWB chip from Qorvo and the BNO085 initial measurement unit (IMU) from CEVA. Meanwhile, a DFROBOT SEN0311 ultrasonic sensor with a measurement accuracy of ±1 cm was integrated into the H-UWB device to measure tree DBH in real time for position correction.

In this study, three types of data were collected as follows: (1) DATA1: measured distances between UWB device pairs within the network coverage area (see Figure 3(a)); (2) DATA2: distances between the H-UWB device and measurable surrounding UWB devices for each tree being mapped (see Figure 3(b)); (3) DATA3: headings of the H-UWB device at the measurement locations, along with the DBHs of the trees (see Figure 3(c)).

This contribution has been peer-reviewed. The double-blind peer-review was conducted on the basis of the full paper.
https://doi.org/10.5194/isprs-annals-XI-1-2026-297-2026 | © Author(s) 2026. CC BY 4.0 License.

During data collection, each tree was measured only once using the H-UWB device mounted on a wooden caliper (see Figure 1), which is sufficient to improve field efficiency. As shown in Figures 1 and 3(c), a gap was maintained between the tree stems and the H-UWB device, which helped reduce measurement interference and thereby improve system accuracy. For each tree, the H-UWB device was positioned at a height of 1.3 m above ground level to collect DATA2 and DATA3. For DATA1, the operator carried the H-UWB device and walked around the test site during which the device triggered surrounding UWB devices to measure pairwise distances. As a result, DATA1, DATA2, and DATA3 were all recorded by the H-UWB device for subsequent data processing and performance evaluation. Additionally, to verify the reliability of the proposed method, two datasets, namely TEST1 and TEST2, were collected by replacing the UWB devices in the test site and repeating the data collection process using the same method.

For field reference, the local position of each tree in the test site, was determined using a Trimble S7 total station (TS) with a direct ranging accuracy of 2 mm, while the diameter at breast height of each tree was measured using a digital caliper from Masser Oy with an accuracy of ±1 mm. The position on the tree surface was first measured and subsequently corrected to the trunk center using the corresponding DBH.

### 2.3 Position Estimation for the Network

To determine the final tree positions, we first estimated the relative positions of all UWB devices in the network. To achieve this, a local coordinate frame was adopted for the UWB network and the H-UWB device. Notably, only 2D positions were considered in this study. The measured distances between UWB1, UWB2, UWB3 and UWB4 were first extracted from DATA1. The position of UWB1 was then set as the origin. The x-axis was defined along the direction from UWB1 to UWB2, and UWB2 was assigned a local position of $(d_{12}, 0)$. Subsequently, the local positions of UWB3 and UWB4 were estimated by solving a nonlinear lease squares problem with the following residuals:

$$\boldsymbol{p}_i = \operatorname{argmin} \sum_{j=1}^{N} (\left\| \boldsymbol{p}_i - \boldsymbol{p}_j \right\|_2 - d_{ij})^2 \tag{1}$$

where $\boldsymbol{p}_i$ is the position of the *i*-th device to be estimated, $\boldsymbol{p}_j$ is the known position of the *j*-th device in the network, and $d_{ij}$ is the measured distance between devices *i* and *j*.

To obtain the local positions of the remaining devices, UWB5 to UWB16, we first identified the devices located within the coverage area of the sub-network formed by UWB1 to UWB4 using DATA1. Specifically, devices with at least three distance measurements to devices UWB1 to UWB4 were selected, and their positions were estimated using the same method as in Eq. (1), as indicated in green in Figure 3. Since the coverage distance of each device exceeded approximately 44 m, it was straightforward to ensure that some devices fell within the coverage area of UWB1 to UWB4. For devices outside this sub-network coverage, corresponding sub-networks were identified, and their positions were subsequently estimated. However, for devices located at the boundary of the network, only two distance measurements to known nodes were available, e.g., devices marked in yellow in Figure 4, resulting in a Geometric Singularity in the position estimation. To address this issue, a map-based constraint strategy was introduced. This approach leverages the preciously estimated network structure to constrain the solution outside the boundary polygon formed by the known nodes. Let $M \subset \mathbb{R}^2$ denote the region enclosed by the polygon defined by the set of vertices $\{\boldsymbol{p}_1, \boldsymbol{p}_2, \ldots, \boldsymbol{p}_n\}$. A target point $\boldsymbol{p} = [x, y]^T$ is constrained by the map as:

$$p \notin M \text{ , or equivalently,}$$

$$\exists k \in \{1, 2, \ldots, K\}, a_k x + b_k y + c_k > 0 \tag{2}$$

where $K$ is the number of edges of the known network boundary polygon formed by the known devices. Figure 3 illustrates the overall framework for estimating the positions of all devices in the network.

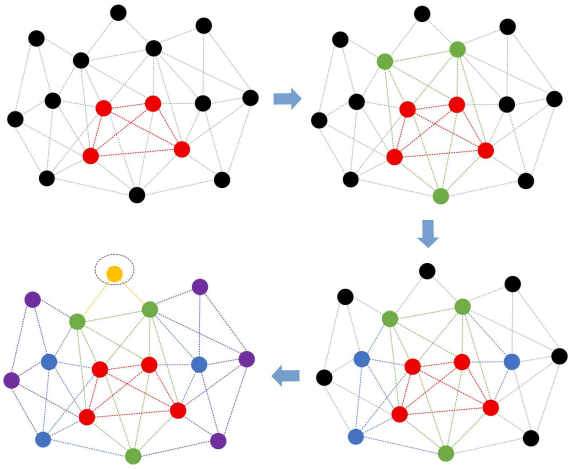

Figure 4. An example of the overall position estimation for the entire network. Red points denote the estimated local positions of UWB1 to UWB4, while green, blue, and pink points correspond to the second, third and fourth round of sub-network estimations, respectively.

Notably, once all devices were deployed in the plot, the entire network behaved as a rigid structure, and all local positions were estimated with respect to distance $d_{12}$. Therefore, inaccurate distance measurement of $d_{12}$ would lead to an inaccurate network, eventually resulting in unexpected errors in the position estimation of tree stems. To address this issue, a fine estimator was further developed to optimize the entire network by minimizing the residual sum of squares of the pairwise distances, which is expressed as:

$$\min \sum_{i \neq j}^{N} (d_{ij} - d'_{ij})^2 \tag{3}$$

where $d'_{ij}$ is the distance computed from the estimated local positions. Specifically, we adjusted $d_{12}$ within a specified distance range and calculated Eq. (2) to find the best value of $d_{12}$, and thus found the best network. In this study, a distance range of $d_{12} \pm 0.3$ m with a step size of 0.01 m was applied based on the findings reported in (Liu et al., 2025).

### 2.4 Tree Localization

As shown in Figure 2(b), the position of the H-UWB device was determined using multilateration based on DATA2, following the same method as in Eq. (1). To obtain the optimal solution of Eq. (1), the least squares method was employed in this study, which can be obtained by

$$\boldsymbol{p} = (\boldsymbol{A}^T \boldsymbol{A})^{-1} \boldsymbol{A}^T \boldsymbol{b} \tag{4}$$

where $\boldsymbol{A} \in \mathbb{R}^{(N-1)\times 2}$ and $\boldsymbol{b} \in \mathbb{R}^{(N-1)}$ are the matrix and vector constructed from the local positions of the known devices surrounding the H-UWB device. In addition, the positioning algorithm was applied to the antenna location of the H-UWB device with respect to the local UWB network. Therefore, to determine the actual positions of individual trees, all measurements were shifted to the centers of tree stems, as illustrated in Figure 2(c). For this purpose, the heading $\theta$ of the H-UWB device with respect to magnetic north during the measurement was used to compute the offsets as follows:

$$\Delta x = d_1 \cdot \cos(360 - \theta) - d_2 \cdot \sin(360 - \theta) \quad (5a)$$

$$\Delta y = d_1 \cdot \sin(360 - \theta) + d_2 \cdot \cos(360 - \theta) \quad (5b)$$

where $d_1 = -(d/2 + d_{offest})$, in which $d$ is the measured DBH of the tree and $d_{offest}$ is a known offset in the x-direction between the antenna location of the UWB receiver and the selected test point of the H-UWB device, and $d_2$ is the known offset in the y-direction. Subsequently, the actual position of the tree stem was obtained as $(x_t, y_t) = (x, y) + (\Delta x, \Delta y)$.

The heading was measured using a BNO085 sensor integrated into the H-UWB device, which provides heading measurements relative to magnetic north with an accuracy of approximately ±3° under typical field conditions. Forest environments are generally free of strong magnetic disturbances; therefore, the heading measurements are only minimally affected. The magnetometer was calibrated in the field using a 3D figure-8 motion according to the manufacturer’s instructions. No additional correction for magnetic declination was applied, and thus, all headings remain referenced to magnetic north. In addition, the heading is applied consistently within the sensor’s coordinate system, with all angles following the same convention (right-handed, yaw defined clockwise from the x-axis of the sensor frame). These implementation details ensure the reproducibility of the method and allow users to account for potential heading uncertainties in field applications.

### 2.5 Evaluation Criteria

To evaluate the measurement accuracy of the proposed method, we first registered the measured tree positions to the field reference using the 2D registration algorithm proposed by Hyyppä et al. (2021). This registration algorithm consists of two parts: a coarse 2D registration applied to identify matching tree pairs among different datasets and a fine registration developed to further optimize the tree locations by integrating the iterative closest point algorithm. As a result, the trees of different datasets would be registered as matching tree pairs by applying suitable parameters in the 2D registration algorithm, including the search radius and registration threshold, as well as the number of tentative matches. As all the reference trees were measured by the H-UWB, we merely minimized the registration threshold to ensure that all measured trees were registered to the field reference. Finally, we employed a search radius of 5 m and a registration threshold of 0.30 m. Subsequently, the measurement accuracy of the proposed method for each tree was obtained by calculating the Euclidean distance between a matched tree and its corresponding reference tree:

$$e_i = \left\| \boldsymbol{p}_i - \boldsymbol{p}_{ref,i} \right\|_2 \quad (6)$$

where $e_i$ = measurement error of the $i$-th tree
$\left\| \boldsymbol{p}_i - \boldsymbol{p}_{ref,i} \right\|_2$ = Euclidean distance
$\boldsymbol{p}_i$ = coordinate of a matched tree stem
$\boldsymbol{p}_{ref,i}$ = coordinate of the corresponding reference tree

The performance of the proposed method was evaluated in terms of precision rather than absolute accuracy due to the absence of GNSS data. In this process, systematic errors in the estimated tree positions were eliminated, assuming that the reference is accurate, whereas such errors would remain in the evaluation of global accuracy based on the field reference. Although no accurate GNSS data were available for the H-UWB dataset, a horizontal plane (parallel to the *xy*-plane) was still performed as part of the georeferencing process to identify matching trees. Finally, the precision of the estimated tree stem positions was evaluated by computing the root-mean-square-error (RMSE) and mean-absolute-error (MAE):

$$RMSE = \sqrt{\frac{1}{N_{\boldsymbol{M}}} \sum_{i \in \boldsymbol{M}} \left\| \boldsymbol{p}_i - \boldsymbol{p}_{ref,i} \right\|_2^2} \quad (7a)$$

$$MAE = \frac{1}{N_{\boldsymbol{M}}} \sum_{i \in \boldsymbol{M}} \left\| \boldsymbol{p}_i - \boldsymbol{p}_{ref,i} \right\|_2 \quad (7b)$$

where $\boldsymbol{M}$ = set of matched trees
$N_{\boldsymbol{M}}$ = number of the matched trees

In addition to the RMSE and MAE, other statistical results were also considered in this study, including the maximum and minimum errors (MAX and MIN), the standard deviation (STD), and the 68% and 95% errors of the cumulative distribution functions (CDF) of set $\boldsymbol{E} = \{e_1, e_2, \ldots, e_N\}$.

## 3. Results and Discussion

Figure 5 shows the distribution of the tree position errors for each tree in both TEST1 and TEST2, and Table I presents the corresponding statistical results. Additionally, Figure 6 shows the tree maps obtained from H-UWB and registered to the TS-based field reference, where the Euclidean distances between H-UWB trees and their corresponding reference trees are also reported. Notably, all tree positions, including both H-UWB estimates and the field reference, were shifted by subtracting the mean TS location for clarity, such that the average position was approximately zero in both x- and y-directions. While we used the Euclidean distance between the measured results and their corresponding reference tree positions to estimate the performance of the proposed method, and therefore, how much the tree positions were shifted was not important.

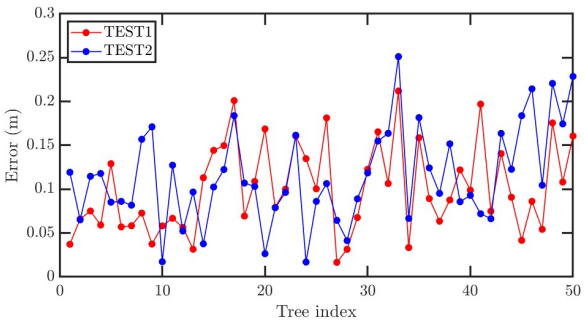


Figure 5. Comparison of the distribution of tree position errors for each tree in TEST1 and TEST2.

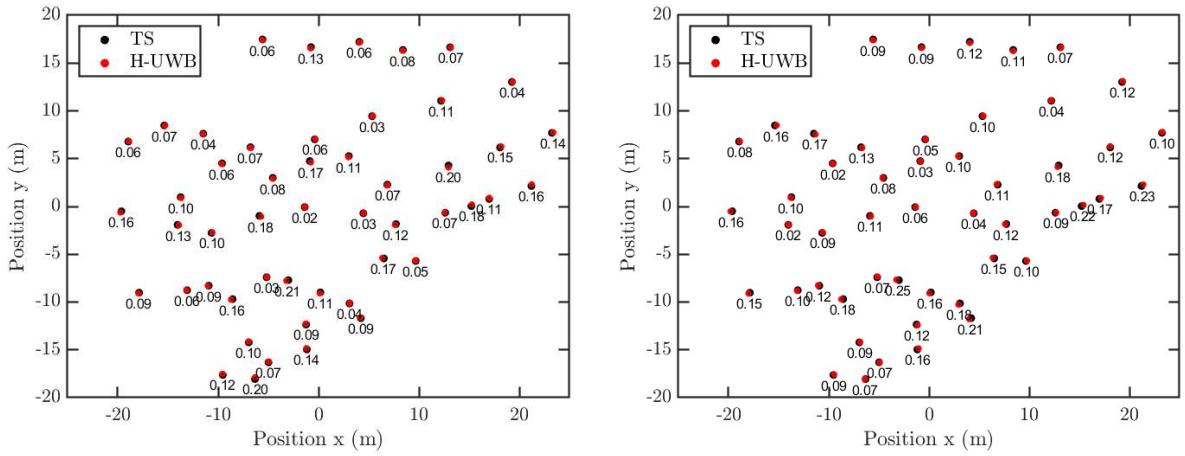


(a) TEST1 (b) TEST2

Figure 6. Tree maps obtained from H-UWB and registered to the field reference, with Euclidean distances between H-UWB trees and their corresponding reference trees. The coordinates are centered at the mean TS tree location for clarity.

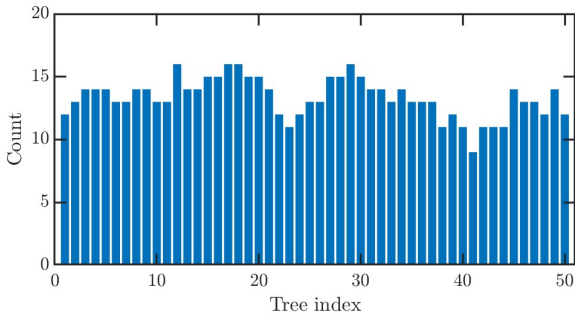


(a) TEST1

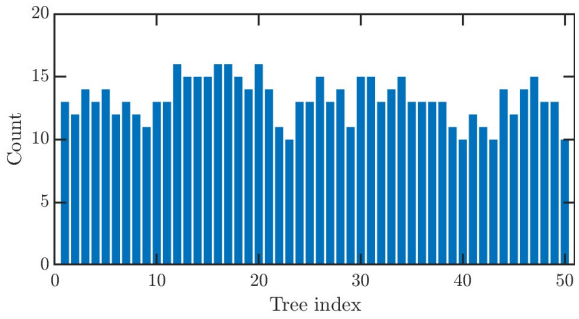


(a) TEST2

Figure 7. Comparison of the count of UWB measurements for each tree in TEST1 and TEST2.

Table I. Statistical results on the precision of the tree positions for TEST1 and TEST2, unit [m].

| Item | RMSE | MAE | MAX | MIN | STD | 68% | 95% |
|---|---|---|---|---|---|---|---|
| TEST1 | **0.11** | **0.10** | 0.21 | 0.02 | 0.05 | 0.12 | 0.20 |
| TEST2 | **0.13** | **0.12** | 0.25 | 0.02 | 0.05 | 0.13 | 0.22 |
| Total | **0.12** | **0.11** | 0.23 | 0.02 | 0.05 | 0.13 | 0.21 |

Based on the results shown in Figure 5 and Table I, the RMSEs and MAEs of the tree positions estimated by the proposed method were 0.11 m and 0.10 m for TEST1, and 0.13 m and 0.12 m for TEST2, respectively. The MAX errors were below 0.25 m, and the 95% errors of the CDF were below 0.22 m, indicating high accuracy of the proposed method.

In addition to the accuracy, the completeness of tree positions within a forest plot is another key factor in providing significant reference information for precision forestry. As shown in Figure 5, the proposed method achieved a completeness of 100%. For commercial MLS or ALS solutions, completeness is typically strongly affected by the point density of the laser sensor used and the performance of the algorithms for tree stem extraction. For example, the completeness of three commonly used commercial MLSs, Deep Forestry from Sweden, Zeb Horizon from GeoSLAM and Hovermap from Emesent, is approximately 86.6%, 90.2% and 96.9%, respectively, while that of the HeliALS is approximately 83.9%, as reported by Muhojoki et al. (2024). Therefore, the proposed method can serve as a strong complement to laser scanner-based approaches for tree position estimation, particularly under forest canopies. Furthermore, for small forest plots, the proposed method can provide a cost-effective and efficient solution while maintaining high efficiency, making it a valuable measure method for precision forestry and environmental sciences.

## 4. Limitations and Applicability

For the proposed method, the performance of UWB technology is the primary factor determining the accuracy of tree position measurements. In addition to the ranging precision of UWB signals under forest canopies, the relative heights of the UWB devices and the overall quality of the UWB network also play important roles. Typically, all UWB devices are assumed to be referenced to the same plane; however, ensuring this is challenging in forest environments with steep slopes or large plots. Theoretically, positioning errors increase as the relative height between devices grows. Since UWB devices are randomly deployed in the forest plot, there is no prior information available to assess the anchor network quality. In small plots, such as the one tested in this study, this issue can be mitigated due to the availability of redundant measurements, as illustrated in Figure. 7. However, for larger areas, e.g., 200 m × 200 m, that exceed the effective coverage of UWB devices, positioning errors may become significant, particularly for devices located near the

network boundaries. This can reduce the accuracy of tree positions and limit the method’s scalability. Advanced algorithms, such as optimizing the network based on the receiver’s trajectory throughout the measurement process, could help address this limitation. Additionally, heading is another factor influencing the measurement accuracy. Fortunately, forest environments are generally free of strong magnetic disturbances, so the heading measurements of most commercially available IMUs are minimally affected once properly calibrated.

## 5. Conclusion

In this study, we present an adaptable method for determining tree positions by integrating heading, diameter at breast height and ultra-wideband technology. The proposed method is simple to implement in forest environments by deploying 16 UWB devices within a plot, with an integrated H-UWB device used to collect data for all trees to be mapped. Experimental results show that the local position of each tree can be determined within a few seconds, with an RMSE of 0.12 m and an MAE of 0.11 m. Although only a simple forest plot was tested in this study, the results demonstrate the potential of the proposed method for advancing research in precision forestry and environmental sciences.

Future work will focus on reducing the number of UWB devices in the network without compromising measurement accuracy, thereby improving field efficiency and reducing system cost. In practical field tests, operators typically prefer to complete data collection using fewer devices while also minimizing the risk of leaving devices behind in the forest. Figure 7 shows the distribution of the number of UWB measurements for each tree in both tests. The results indicate that at least nine UWB measurements were obtained for each tree, demonstrating that the number of measurements was more than sufficient. Typically, three or four high-quality UWB measurements are enough to estimate the target position though multilateration.

## Acknowledgments

This work was supported by funds granted by the Research Council of Finland (RCF) through the UNITE Flagship (359175), projects Diversity4Forests (338644), HPC_Carbon (359203) and Quality4Trees (334002), by the Ministry of Agriculture and Forestry of Finland and European Union NextGenerationEU through the project IlmoStar (VN/27353/2022), and by the Academy Research Fellowships through the project EATP4Plots (368564). The tests were done at ScanForest research infrastructure supported by the RCF (346382).

## References

Anderson, C., Volos, H., Buehrer, R., 2013. Characterization of low-antenna ultrawideband propagation in a forest environment. IEEE Trans Veh Technol, 62, 2878–2895.

Apostol, B., Chivulescu, S., Ciceu, A., Petrila, M., Pascu, I.S., Apostol, E.N., Leca, Ş., Lorenţ, A., Tănase, M., Badea, O., 2018. Data collection methods for forest inventory: A comparison between an integrated conventional equipment and terrestrial laser scanning. Ann For Res, 61, 189–202.

Edson, C., Wing, M.G., 2012. Tree location measurement accuracy with a mapping-grade GPS receiver under forest canopy. Forest Science, 58, 567–576.

Farid Fauzi, M., Hawani Idris, N., Hafiz Yahya, M., Hassan Md Din, A., 2016. Tropical forest tree positioning accuracy: A comparison of low cost GNSS-enabled devices, International Journal of Geoinformatics.

Hyyppä, E., Kukko, A., Kaartinen, H., Yu, X., Muhojoki, J., Hakala, T., Hyyppä, J., 2022. Direct and automatic measurements of stem curve and volume using a high-resolution airborne laser scanning system. Science of Remote Sensing, 5.

Hyyppä, E., Muhojoki, J., Yu, X., Kukko, A., Kaartinen, H., Hyyppä, J., 2021. Efficient coarse registration method using translation- and rotation-invariant local descriptors towards fully automated forest inventory. ISPRS Open Journal of Photogrammetry and Remote Sensing 2, 100007.

Kai, D., Steve, O., Grzegorz, J., Charles, K.T., Dorota, A.G.-B., 2015. UWB for navigation in GNSS compromised environments. Proceedings of the 28th International Technical Meeting of the Satellite Division of The Institute of Navigation (ION GNSS+ 2015) 2380–2389.

Keefe, R.F., Wempe, A.M., Becker, R.M., Zimbelman, E.G., Nagler, E.S., Gilbert, S.L., Caudill, C.C., 2019. Positioning methods and the use of location and activity data in forests. Forests.

Larsson, M., 2022. Localization using distance geometry minimal solvers and robust methods for sensor network self-calibration (Thesis). Lund University.

Li, S., Chen, X., Sun, Y., Lv, C., Yuan, F., Fang, L., 2023. Method and device for measuring the diameter at breast height and location of trees in sample plots. Forests,14.

Liu, Z., Kaartinen, H., Hakala, T., Hyyti, H., Hyyppa, J., Kukko, A., Chen, R., Vastaranta, M., 2025b. Ultra-Wideband-Based Method for Measuring Tree Positions with Decimeter-Level Accuracy Under a Forest Canopy. IEEE J Sel Top Appl Earth Obs Remote Sens.

Luoma, V., Saarinen, N., Wulder, M.A., White, J.C., Vastaranta, M., Holopainen, M., Hyyppä, J., 2017. Assessing precision in conventional field measurements of individual tree attributes. Forests, 8.

Muhojoki, J., Hakala, T., Kukko, A., Kaartinen, H., Hyyppä, J., 2024. Comparing positioning accuracy of mobile laser scanning systems under a forest canopy. Science of Remote Sensing, 9.

Sun, L., Feng, Z., Shao, Y., Wang, L., Su, J., Ma, T., Lu, D., An, J., Pang, Y., Fahad, S., Wang, W., Wang, Z., 2023. The development of a set of novel low cost and data processing-free measuring instruments for tree diameter at breast height and tree position. Forests 14.

Wilkes, P., Lau, A., Disney, M., Calders, K., Burt, A., Gonzalez de Tanago, J., Bartholomeus, H., Brede, B., Herold, M., 2017. Data acquisition considerations for Terrestrial Laser Scanning of forest plots. Remote Sens Environ, 196, 140–153.

Yuan, F., Chen, S., Fang, L., Zheng, S., Liu, Y., Ren, J., 2021. A Method to Locate Tree Positions Using Ultrawideband Technology. J Sens 2021.